

Direct measurements of quantum states by exploiting diffused photon state

KyeoReh Lee¹ and YongKeun Park¹

¹Department of Physics, Korea Advanced Institute of Science and Technology, Daejeon 34141, Republic of Korea.

Email: yk.park@kaist.ac.kr

Measuring the state of a physical system provides a complete understanding of the past, present, and future behavior of the system. Accordingly, techniques for measuring intact physical states are required in all subfields of physics. In quantum systems, however, measuring the exact state of a system is a challenging task due to the complex and uncertain nature of quantum systems¹. The conventional way of measuring a quantum state is the quantum tomographic approach²⁻⁵. However, this is a challenging task because of the extreme vulnerability of the interferometric setup. Recently, direct measurement of a quantum state was realized utilizing the weak measurement⁶⁻¹³. Though this alleviates the difficulty of measuring quantum states, the introduction of a pointer state still limits the generality of the technique. Here, we propose a general but straightforward measurement technique for the quantum state of a photon. At the heart of our idea is an optical diffuser. Based on the random feature of the diffused state, we theoretically show that the density matrix of a photon can be directly reconstructed from a single intensity image after the diffuser. In experimental demonstrations, we successfully measured the density matrices in the position-polarization basis for both pure and mixed states of photons.

The wave function $|\psi\rangle$ is the best way to describe a pure quantum state¹⁴. Although it is still impossible to predict the exact outcomes of quantum measurements, unlike classical mechanics, the wave function helps to explain the evolution and interference of quantum states. In mixed states cases, however, quantum systems are described by more than two individual microstates. In such cases the density operator $\hat{\rho}$ is introduced to characterize both the pure and mixed states in a single form without ambiguity.

For photons, the standard tool for measuring the density matrix is quantum state tomography (QST)²⁻⁴. In QST, to reconstruct the density matrix of a given quantum system, the marginal distributions of the Wigner function are measured using different phases of a local oscillator. Though QST provides the surest way to measure the quantum state of photons, its complicated experimental setups and reconstruction algorithms increase the practical difficulty of quantum state measurement.

Recently, a rather simple and elegant way of determining a quantum state has been proposed – the direct measurement techniques⁶⁻¹². The direct measurement techniques utilize the ‘weak measurement’ in order to relax the quantum uncertainty, and this enables the simultaneous observation of noncommuting operators such as $[\hat{r}, \hat{p}] = i\hbar$. While the weak measurement is an ingenious technique, the introduction of a pointer (or ancilla) state limits its scope of application¹³. Further, the weak measurement is not the only way to achieve direct measurement; for example, direct measurement can also be achieved using sets of strong measurements¹⁵.

Here, we suggest a next generation direct measurement techniques which enables an even simpler and more straightforward quantum states measurement of a photon. The core of the idea is an optical diffuser, which ‘diffuses’ the photon in a random way. Exploiting the randomness of a diffused state, we theoretically show that the density matrix can be directly reconstructed from a single measurement. We

also experimentally prove the versatility of the proposed idea for the position-polarization state of photons in both pure and mixed states.

Let us suppose that an ensemble of pure state photons $|\psi\rangle = \sum_{p=1}^N \langle p|\psi\rangle |p\rangle$ is prepared, where $|p\rangle$ represents a transversal momentum state. In order to determine the quantum state of the photon, an optical diffuser and a camera are placed in series (Fig. 1a).

In general, the functions of optical elements can be described by the scattering operator \hat{S} ^{16,17}. For example, the scattering matrix $S_{xp} = \langle x|\hat{S}|p\rangle$ of a beam splitter and a lens are shown in Figs. 1b and 1c, respectively. Since the S_{xp} is based on the geometric shape of the optical elements, the scattering matrix of a diffuser can be determined in a similar way. (Fig. 1d)¹⁸⁻²⁰. However, unlike ordinary optical elements, the S_{xp} of a diffuser is completely scrambled in order to achieve the ‘diffusion’ of light. Therefore, the diffused state $|\beta\rangle = \hat{S}|\psi\rangle$ over the position basis $|x\rangle$, $\beta_x = \sum_{p=1}^N \langle p|\psi\rangle S_{xp}$ exhibits a Gaussian random distribution called a speckle field^{21,22} (Fig. 1e). Note that the $|\beta\rangle$ is firm and reproducible for identical $|\psi\rangle$ as long as the diffuser remains static. Finally, the measured intensity image I_x for the M position states $|x\rangle$ (or pixels) becomes $\beta_x^* \beta_x$, which is called a speckle pattern.

Now, we define the Z-matrix, which is introduced as a speckle-correlation scattering matrix in Ref.²³,

$$Z_{kl} = \frac{1}{\sigma_k \sigma_l} \left[\langle S_{xk}^* S_{xl} \beta_x^* \beta_x \rangle_x - \langle S_{xk}^* S_{xl} \rangle_x \langle \beta_x^* \beta_x \rangle_x \right], \quad (1)$$

where $\langle \rangle_x = \frac{1}{M} \sum_{x=1}^M$, and $\sigma_p = \langle S_{xp}^* S_{xp} \rangle_x$ are the normalization coefficients. Notice that Eq. (1) can be directly calculated from the intensity image of the diffused state $\beta_x^* \beta_x$. Because of the Gaussian random behavior of S_{xp} and β_x over the $|x\rangle$ space, we determine that Eq. (1) can be expanded using Wick’s theorem²⁴,

$$Z_{kl} = \frac{1}{\sigma_k \sigma_l} \left[\langle S_{xk}^* \beta_x \rangle_x \langle S_{xl} \beta_x^* \rangle_x + \langle S_{xk}^* \beta_x^* \rangle_x \langle S_{xl} \beta_x \rangle_x \right]. \quad (2)$$

When the number of samplings (or camera fields-of-view) is large enough to satisfy $M \gg N$, the general orthogonality relations $\sqrt{\frac{1}{\sigma_k \sigma_l}} \langle S_{xk}^* S_{xl} \rangle_x = \delta_{kl}$ and $\langle S_{xk}^* S_{xl} \rangle_x = 0$ hold for Gaussian random variables²². Then, the Z-matrix becomes

$$Z_{kl} = \langle p_k | \psi \rangle \langle \psi | p_l \rangle, \quad (3)$$

which is the *density matrix* of the initial quantum state in momentum space $\rho_{p,s}$. Although we derived Eq. (3) for pure photon states for simplicity, this is also generally valid in the case of mixed photon states (see Methods).

In addition, the proposed idea can be easily extended to the polarization (spin) state of a photon by imparting polarization distinguishability to the diffuser (e.g., a polarizing beam splitter). Then, the

scattering matrix is also extended to the polarization states $S_{xp,s} = \langle x | \hat{S} | p, s \rangle$; and according to the theory, the position and polarization states of photons can be simultaneously measured from a single intensity image.

To experimentally demonstrate the proposed idea, we prepared a compact unit assembled with a camera (Fig. 2a). The unit was composed of only three optical components – an iris, a diffuser, and a polarizer. The iris is added before the diffuser in order to block ambient light, and the polarizer is inserted to fix the detection polarization state. The distance between the diffuser and the camera is adjusted to assign a single position state $|x\rangle$ for each pixel in the camera (i.e., diffraction limit \cong pixel size).

In order to maximize the polarization-position coupling of the diffuser, we deposited rutile nanoparticles (particle size ≤ 100 nm) on a coverslip using a spray painting method (Fig. 2b, see Methods). Due to the high birefringence ($\Delta n = 0.288$ for 633 nm)²⁵ and multiple scattering of the custom rutile diffuser, the diffused state is completely depolarized regardless of the initial polarization state of a photon.²⁶ The scattering matrix $S_{xp,s}$ of the rutile diffuser is calibrated using SLM and Michelson type interferometry (see Methods)^{23,27}. A total of 44×40 transversal momentum states in both the $|p, H\rangle$ and $|p, V\rangle$ states ($N = 3,520$), and 512×512 central camera pixels ($M = 262,144$) were utilized as the input and output bases, respectively (Fig. 2c).

For the first demonstration, we prepared the pure quantum states by placing the polarizer in front of the laser source (Fig. 2a). Using a spatial light modulator (SLM) and a quarter-wave plate, the desired position-polarization state of a photon was prepared. Notice that the polarization state of the prepared photon depends on the phase of the SLM φ_{SLM} . Since the φ_{SLM} changes over the SLM active area, the polarization state also depends on the transversal position, which is sometimes called the ‘vector beam’ (Fig. 2a, see Methods)²⁸.

Next, we reconstructed the density matrices from the captured intensity images I_x (Fig. 3a) based on the proposed theory. Since the proposed method is always accompanied by a fundamental error source – the second term in Eq. (2) - we utilized an additional error reduction algorithm to enhance the accuracy of the results (see Methods)²³. In particular, when M/N is not sufficient, the additional sequences are required to minimize the error. Note that since the additional sequence does not require any additional information or free variable, the generality of our method is not lost.

The reconstructed density matrices are depicted in Fig. 3b. The transversal position $|r\rangle$ basis is used rather than the momentum $|p\rangle$ basis for a more intuitive visualization. Using the eigenvector analysis of the density matrix, the complex valued wave function $|\psi\rangle$ is retrieved (Fig. 3c). Further, φ_{SLM} can be inferred from the polarization analysis over $|r\rangle$. The reconstructed azimuthal vector beam is shown in Fig. 3d. We found there was good agreement between the expected and measured φ_{SLM} (Figs. 3e and 3f).

In order to test the versatility of the proposed method, we prepared mixed states of photons as the next demonstration. The overall experimental setup was unchanged, but the polarizer in front of the laser was removed (Fig. 2a). The mixed state of photons generated from the laser was confirmed by measuring the Stokes parameters (see Methods). Since the SLM with a quarter-wave plate modulates

$|R\rangle$ polarization states only, the prepared photon states are expected to be $\hat{\rho} = \frac{1}{2}|\psi_L\rangle\langle\psi_L| + \frac{1}{2}|\psi_R\rangle\langle\psi_R|$, where $|\psi_L\rangle$ and $|\psi_R\rangle$ are two orthonormal wave functions in the $|L\rangle$ and $|R\rangle$ polarization states, respectively.

Following the same procedure as used in the case of pure photon states, the density matrix (Fig. 4b) can be reconstructed from the captured I_x (Fig. 4a). In order to clearly show the measured mixed state, the basis of the density matrix was transformed from $|HV\rangle$ to $|LR\rangle$. As expected, the coherence terms between $|L\rangle$ and $|R\rangle$ states were eliminated (Fig. 4c). Further, using an eigenvector analysis, the complex valued $|\psi_L\rangle$ and $|\psi_R\rangle$ were retrieved with their corresponding statistical probabilities $P_L = 0.48$ and $P_R = 0.52$ (Fig. 4d). Note that only the phase of the $|R\rangle$ polarization state is modulated, and it should be the φ_{SLM} . Again, we found good agreement between the expected and measured φ_{SLM} (Figs. 4e and 4f).

For the mixed states, however, we found that the speckle pattern I_x exhibited lower visibility due to the incoherent summation of microstates. This would be an issue when the dimension of the basis increases. In such cases, one may require a greater number of samplings with better dynamic range to reconstruct a reliable density matrix.

In this work, we successfully characterized the full position-polarization state of a photon using an optical diffuser. To characterize the entire quantum state of the photon, however, the photon number (Fock) states $|n\rangle$ must be additionally considered.

In theory, it is possible to extend the proposed method to the number states. By employing the photon number-position coupling (e.g., nonlinear effects) to a diffuser, the number state can also be distinguished by the speckle pattern in a similar way. Unfortunately, the practical photon number sensitivity of a nonlinear diffuser would be an issue for the experimental demonstrations.

We have to emphasize that the proposed method is solely based on the *randomness* which is simply introduced by an optical diffuser. If we replace a diffuser with a lens, as in Fig. 1a, it becomes a single lens camera, and the intensity image I_x is a photograph, which obviously does not have phase information in it. This work shows that selecting a randomized sampling basis can be a powerful method for retrieving complex valued quantities from simple intensity measurements. We expect that the present method proposes a new avenue in various quantum-related fields such as quantum information theory, quantum computing, and quantum cryptography by employing the randomness upon the quantum state measuring part.

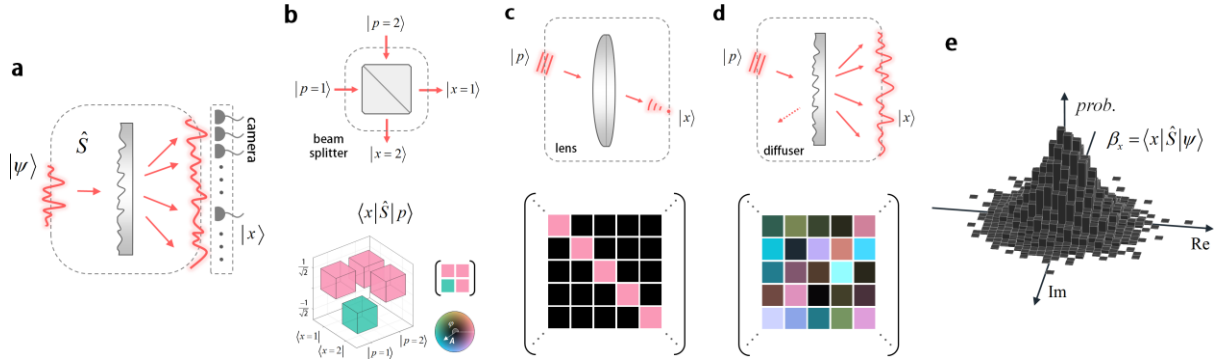


Figure 1 | Idea overview. **a**, The proposed quantum state measuring apparatus consists of an optical diffuser and a camera. **b-d**, Scattering matrices $\langle x|\hat{S}|p\rangle$ of a beam splitter (b), a lens (c), and a diffuser (d). Strictly speaking, every possible output photon state has to be considered in the entire scattering matrix including the reflective portion. Therefore, the S_{xp} in (d) is a part of the scattering matrix, which does not have to be square nor unitary. In the color circle, the A and φ denote the amplitude and phase of the complex value in arbitrary and radian units, respectively. **e**, the Gaussian probability distribution of the speckle field, $|\beta\rangle$ over the transversal position space $|x\rangle$.

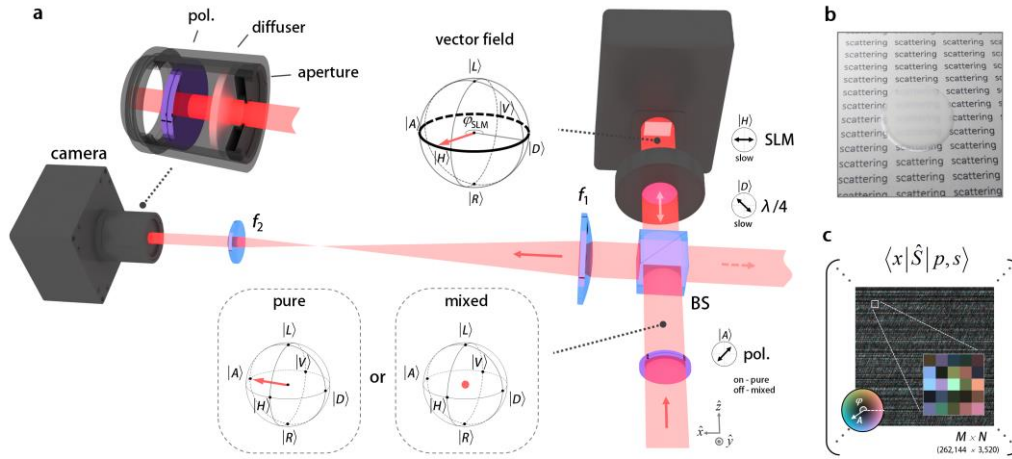


Figure 2 | Experimental setup. **a**, The optical setup for preparing and measuring the quantum state of photons. Using a polarizer with an unpolarized laser (wavelength, 633 nm) The initial polarization state of a photon is set to either $|A\rangle = \frac{1}{\sqrt{2}}|H\rangle - \frac{1}{\sqrt{2}}|V\rangle$ or $\frac{1}{2}|H\rangle\langle H| + \frac{1}{2}|V\rangle\langle V|$ for a pure or mixed state, respectively. In the case of the pure state, the output polarization state is a function of φ_{SLM} , which varies over the SLM active area. Therefore, the position and polarization states of an output photon are coupled. In the case of the mixed state, the SLM phase pattern only modulates the $|R\rangle = \frac{1}{\sqrt{2}}|H\rangle - \frac{1}{\sqrt{2}}i|V\rangle$ polarization state of a photon. **b**, A custom-made diffuser made of rutile nanoparticles; the rutile nanoparticles were deposited on the 25 mm diameter coverslip by a spray painting method. **c**, Calibrated scattering matrix $S_{xp,s}$ of the rutile diffuser. Within the calibrated M -by- N matrix ($262,144 \times 3,520$), the central 512×512 part is displayed. In the color circle, the A and φ denote the amplitude and phase of the complex value in arbitrary and radian units, respectively.

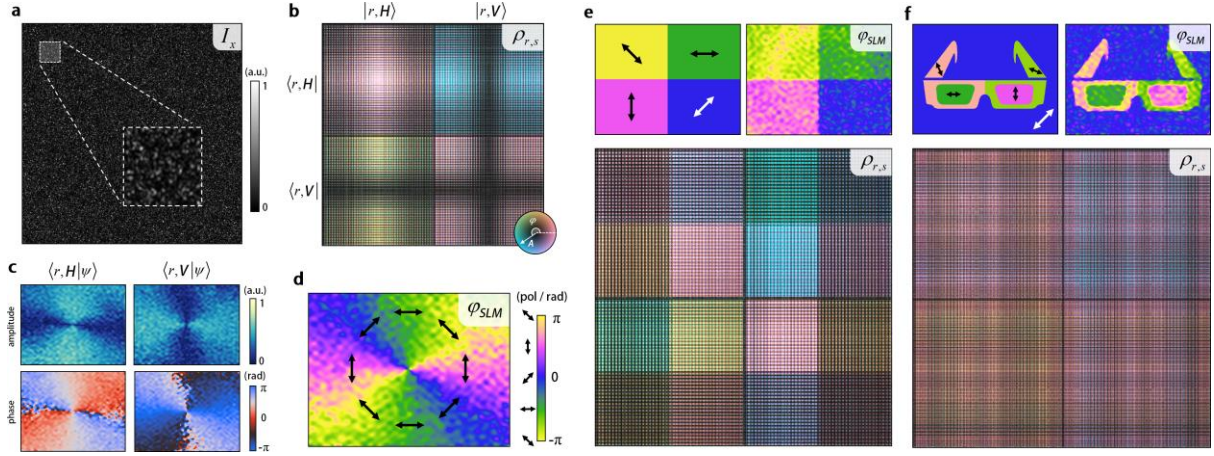


Figure 3 | Pure state of photons. **a**, The raw image of the diffused state of a photon, I_x measured from the camera. **b**, The retrieved N -by- N ($3,520 \times 3,520$) density matrix $\rho_{r,s}$ based on the proposed method. Note that the $|r\rangle$ basis is used for better visualization, instead of the $|p\rangle$ basis, by Fourier transform. In the color circle, the A and φ denote the amplitude and phase of the complex value in arbitrary and radian units, respectively. **c**, The wave function of a photon $|\psi\rangle$ calculated from the measured density matrix is represented over the $|r\rangle$ space in both $|H\rangle$ and $|V\rangle$ polarization. **d**, Visualization of the position-dependent polarization of the measured photon, which is related to the input SLM phase φ_{SLM} pattern. **e, f**, Reconstructed density matrices (bottom), and the corresponding φ_{SLM} patterns (top right) are displayed with the input φ_{SLM} patterns (top left).

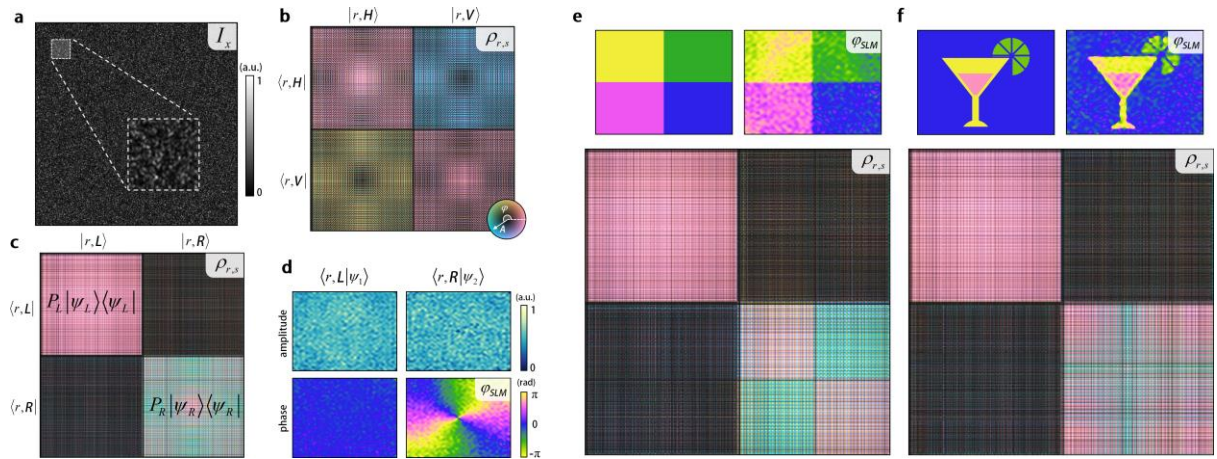


Figure 4 | Mixed state of photons. **a**, The raw image of the diffused state of a photon, I_x measured from the camera. **b**, Retrieved density matrix $\rho_{r,s}$ based on the proposed method, represented in the $|HV\rangle$ polarization basis. In the color circle, the A and φ denote the amplitude and phase of the complex value in arbitrary and radian units, respectively. **c**, Identical density matrix with (b) represented in the $|LR\rangle$ polarization basis. Note that the coherence terms are eliminated. Here, $P_L = 0.48$ and $P_R = 0.52$ are the measured statistical probabilities of $|\psi_L\rangle$ and $|\psi_R\rangle$, respectively. **d**, The two orthonormal wave functions of a mixed state photon $|\psi_L\rangle$ and $|\psi_R\rangle$, calculated from the measured density matrix is represented in the $|L\rangle$ and $|R\rangle$ polarizations, respectively. Note that only the phase

of the $|R\rangle$ polarization is modulated by the SLM. **e, f**, Reconstructed density matrices in the $|L\rangle|R\rangle$ polarization basis (bottom), and the corresponding φ_{SLM} patterns (top right) are displayed with the input φ_{SLM} patterns (top left). The measured statistical probabilities are equal to (c) for both (e) and (f), within ± 0.03 range.

Methods

Density matrix measurement for mixed states.

Let us suppose an ensemble of the mixed state photons, $\hat{\rho} = \sum_j P_j |\psi_j\rangle\langle\psi_j|$ are prepared, where P_j denotes the statistical probability of $|\psi_j\rangle$. After the diffuser, each pure state $|\psi_j\rangle$ produces a different diffused field $\beta_{x,j} = \langle x | \hat{S} | \psi_j \rangle$, and the acquired intensity image I_x would be the incoherence summation of speckle patterns $I_x = \sum_j P_j \beta_{x,j}^* \beta_{x,j}$.

Substituting the measured intensity image into Eq. (1), the Z-matrix for the mixed states is

$$Z_{kl} = \sum_j P_j z_{kl,j}, \quad (4)$$

where $z_{kl,j}$ is the individual Z-matrix of the pure state $|\psi_j\rangle$ based on Eq. (1). Since each $z_{kl,j}$ follows Eqs. (2) and (3) separately, Eq. (4) becomes

$$Z_{kl} = \sum_j P_j \langle p_k | \psi_j \rangle \langle \psi_j | p_l \rangle, \quad (5)$$

which is the density matrix of the mixed state in the momentum basis. Please find the MATLAB codes in the Supplementary Methods.

Rutile diffuser manufacturing

A rutile diffuser was introduced in order to maximize the depolarization character, without sacrificing light transmissivity. The custom rutile paint was made by mixing rutile nanoparticles (637262, Sigma-Aldrich Co. LLC.) with resin (RSN0806, DOW CORNING®) and solvent (toluene, 99%) in a proper ratio (0.5 g : 1 mL : 10 mL). In order to disperse the rutile nanoparticles, we sonicated the paint for 10 min. The rutile paint was deposited on both sides of the 25 mm diameter round coverslip by the spray painting method using a commercial air brush (DH-125, Sparmax). After the spray painting, the diffuser was baked (100°C, 10 min) to cure the resin.

Scattering matrix calibration

Supplementary Fig. 1 shows the experimental setup for the scattering matrix calibration. The scattering matrix $S_{xp,s}$ is the collection of corresponding diffused photon states for the $|p,s\rangle$ states measured in the $|x\rangle$ space. Therefore, we produced the $|p,s\rangle$ photon states using a SLM (X10468-01, Hamamatsu photonics K.K.) and a liquid crystal variable retarder (LCVR; LCC1222-A, Thorlabs Inc.).

The transversal momentum states of the photon $|p\rangle$ were prepared by displaying phase ramps (or plane waves) on the SLM. We selected a 44×40 central area of the reciprocal domain of the SLM. The

allocated transversal momentum for the $|p = n\rangle$ state was the n -th component of a vectorized 44×40 matrix (Supplementary Fig. 2). The polarization state of photon $|s\rangle$ was prepared by the LCVR by adjusting the phase retardance. Since our SLM only modulates the $|H\rangle$ polarization state, we achieved output polarization states $|H\rangle$ and $|V\rangle$ for 0 and $\frac{\lambda}{2}$ phase retardation, respectively. Therefore, a total of $44 \times 40 \times 2$ ($N = 3,520$) $|p, s\rangle$ states were prepared in our experiments.

In order to measure the complex numbers $S_{xp,s}$, we constructed a Michelson type interferometer using a He-Ne laser (HNL050R, Thorlabs Inc.). The reference arm supplied a static diffused state on the $|x\rangle$ space, called a reference speckle field $\gamma_x = \langle x | \hat{S} | \gamma \rangle$, where $|\gamma\rangle$ denotes the position-polarization state of the reference arm.

Using the phase shifting concept, we achieved the interference term $\gamma_x^* S_{xp,s}$. For each $|p, s\rangle$ input state, we took three images I_0 , I_1 , and I_2 , while the SLM displayed $|p, s\rangle$, $|p, s\rangle e^{i\frac{2\pi}{3}}$, and $|p, s\rangle e^{-i\frac{2\pi}{3}}$, respectively. Then, the interference term can be calculated as follows: $\gamma_x^* S_{xp,s} = \frac{1}{3} \left[I_0 + I_1 e^{-i\frac{2\pi}{3}} + I_2 e^{i\frac{2\pi}{3}} \right]$ ²⁹. The additional γ_x^* term must be considered during the calculation of the density matrices. Fortunately, we found the phase part of γ_x^* was automatically erased out when we constructed the Z-matrix in Eq. (1).

On the other hand, the amplitude part of γ_x^* remained as a form of $|\gamma_x|^2$, but was compensated by one additional measurement while the sample arm was blocked. As a result, we took a total of $3N+1$ (10,561) images to calibrate the TM; it required about 19 minutes.

We took the central 512×512 pixels ($M = 262,144$) of the CCD camera ($4,242 \times 2,830$ pixels; 3.1mm pitch; MD120MU-SY, XIMEA GmbH) for position states $|x\rangle$. Although a greater number of sampling position states provides better results by suppressing the second term in Eq. (2), we could not fully utilize all of the CCD pixels because of limited data storage capacity, and the computing ability of the used computer (3.50 GHz, intel® core™ i5-4690 CPU; 32.0 GB RAM).

Vector field generation

For the pure photon states, the initial polarization state of photon was prepared to be $|A\rangle = \frac{1}{\sqrt{2}}|H\rangle - \frac{1}{\sqrt{2}}|V\rangle$, or $\frac{1}{\sqrt{2}} \begin{pmatrix} 1 \\ -1 \end{pmatrix}$. Since $|A\rangle$ is the fast axis of the quarter-wave plate, the polarization state was maintained before the SLM. The SLM modulates $|H\rangle$ polarization; therefore, the reflected polarization state is $\frac{1}{\sqrt{2}} \begin{pmatrix} e^{i\varphi} \\ 1 \end{pmatrix}$, where φ denotes the delayed phase from a single pixel of SLM. Note that the sign of $|V\rangle$ is changed due to the reflection geometry of the SLM, $(x, y, z) \rightarrow (x, -y, -z)$. After the quarter-wave plate, the output polarization state becomes:

$$|s\rangle_\varphi = e^{i\frac{\varphi}{2}} \begin{pmatrix} \cos\left(\frac{\varphi}{2} + \frac{\pi}{4}\right) \\ \sin\left(\frac{\varphi}{2} + \frac{\pi}{4}\right) \end{pmatrix}. \quad (6)$$

Allocating different phase values for each pixel, the output photon state exhibits a position dependent polarization state called the ‘vector field.’

Error reduction iterative algorithm

To suppress fundamental errors and practical noises, we utilized the Gerchberg-Saxton (GS) type iterative algorithm³⁰, while the Fourier transform in the original GS algorithm was replaced by the scattering operator of the diffuser \hat{S} .

For each iteration step, the algorithm consists of three sub-steps. First, the diffused photon state $\rho_x = S_{xp,s} \rho_{p,s} S_{xp,s}^+$ is calculated, where $S_{xp,s}^+$ is the pseudoinverse of $S_{xp,s}$. Second, ρ_x is updated to ρ_x^\bullet utilizing the measured intensity image I_x as a constraint. The amplitude part of ρ_x is revised, while the phase part is conserved. Third, the $\rho_{p,s}$ is updated to $\rho_{p,s}^\bullet = S_{xp,s}^+ \rho_x^\bullet S_{xp,s}$. The iteration starts from the retrieved density matrix from Eq. (3), and stops when the density matrix converges; the correlation between $\rho_{p,s}$ and $\rho_{p,s}^\bullet$ reaches 0.999998. In conclusion, the iterative algorithm reduces error by converging the closest local minimum for a given intensity image I_x starting from the initial reconstruction, Eq. (3). Note that this iterative algorithm does not require any additional information or free variables. Please find the MATLAB codes in the Supplementary Methods.

Stokes parameters measurements

In order to confirm the polarization state of photons that were generated from a He-Ne laser (HNL050R, Thorlabs Inc.), we measured the Stokes parameter by measuring the power of six different polarization states. The measuring polarization was changed using a polarizer (LPVISE100-A; Thorlabs Inc.) and a liquid crystal variable retarder (LCVR; LCC1222-A, Thorlabs Inc.). The measured Stokes parameters were (1, 0.006, -0.004, -0.006), which indicates the unpolarized state of the photons.

References:

- 1 Pauli, W., Achuthan, P. & Venkatesan, K. *General Principles of Quantum Mechanics*. (Springer Berlin Heidelberg, 2012).
- 2 Smithey, D. T., Beck, M., Raymer, M. G. & Faridani, A. Measurement of the Wigner distribution and the density matrix of a light mode using optical homodyne tomography: Application to squeezed states and the vacuum. *Physical Review Letters* **70**, 1244-1247 (1993).
- 3 Breitenbach, G., Schiller, S. & Mlynek, J. Measurement of the quantum states of squeezed light. *Nature* **387**, 471-475 (1997).
- 4 Leonhardt, U. *Measuring the Quantum State of Light*. (Cambridge University Press, 1997).
- 5 Lvovsky, A. I. *et al.* Quantum State Reconstruction of the Single-Photon Fock State. *Physical Review Letters* **87**, 050402 (2001).
- 6 Lundeen, J. S., Sutherland, B., Patel, A., Stewart, C. & Bamber, C. Direct measurement of the quantum wavefunction. *Nature* **474**, 188-191 (2011).
- 7 Kocsis, S. *et al.* Observing the Average Trajectories of Single Photons in a Two-Slit Interferometer. *Science* **332**, 1170 (2011).
- 8 Lundeen, J. S. & Bamber, C. Procedure for Direct Measurement of General Quantum States Using Weak Measurement. *Physical Review Letters* **108**, 070402 (2012).
- 9 Salvail, J. Z. *et al.* Full characterization of polarization states of light via direct measurement. *Nature Photonics* **7**, 316-321 (2013).
- 10 Malik, M. *et al.* Direct measurement of a 27-dimensional orbital-angular-momentum state vector. *Nature Communications* **5**, 3115 (2014).

- 11 Thekkadath, G. S. *et al.* Direct Measurement of the Density Matrix of a Quantum System. *Physical Review Letters* **117**, 120401 (2016).
- 12 Piacentini, F. *et al.* Measuring Incompatible Observables by Exploiting Sequential Weak Values. *Physical Review Letters* **117**, 170402 (2016).
- 13 Dressel, J., Malik, M., Miatto, F. M., Jordan, A. N. & Boyd, R. W. Colloquium: Understanding quantum weak values: Basics and applications. *Reviews of Modern Physics* **86**, 307 (2014).
- 14 Fano, U. Description of States in Quantum Mechanics by Density Matrix and Operator Techniques. *Reviews of Modern Physics* **29**, 74-93 (1957).
- 15 Vallone, G. & Dequal, D. Strong Measurements Give a Better Direct Measurement of the Quantum Wave Function. *Physical Review Letters* **116**, 040502 (2016).
- 16 Heisenberg, W. Die „beobachtbaren Größen“ in der Theorie der Elementarteilchen. *Zeitschrift für Physik* **120**, 513-538 (1943).
- 17 Nieto-Vesperinas, M. *Scattering and Diffraction in Physical Optics*. (2006).
- 18 Popoff, S. M. *et al.* Measuring the Transmission Matrix in Optics: An Approach to the Study and Control of Light Propagation in Disordered Media. *Physical Review Letters* **104**, 100601 (2010).
- 19 Vellekoop, I. M. & Mosk, A. P. Focusing coherent light through opaque strongly scattering media. *Opt. Lett.* **32**, 2309-2311 (2007).
- 20 Mosk, A. P., Lagendijk, A., Lerosey, G. & Fink, M. Controlling waves in space and time for imaging and focusing in complex media. *Nature Photonics* **6**, 283-292 (2012).
- 21 Goodman, J. W. *Speckle Phenomena in Optics: Theory and Applications*. (Roberts & Company, 2007).
- 22 Goodman, J. W. *Statistical Optics*. (Wiley, 2015).
- 23 Lee, K. & Park, Y. Exploiting the speckle-correlation scattering matrix for a compact reference-free holographic image sensor. *Nature Communications* **7**, 13359 (2016).
- 24 Wick, G. C. The Evaluation of the Collision Matrix. *Physical Review* **80**, 268-272 (1950).
- 25 DeVore, J. R. Refractive Indices of Rutile and Sphalerite. *J. Opt. Soc. Am.* **41**, 416-419 (1951).
- 26 Park, J., Park, J.-H., Yu, H. & Park, Y. Focusing through turbid media by polarization modulation. *Opt. Lett.* **40**, 1667-1670 (2015).
- 27 Yoon, J., Lee, K., Park, J. & Park, Y. Measuring optical transmission matrices by wavefront shaping. *Opt. Express* **23**, 10158-10167 (2015).
- 28 Zhan, Q. Cylindrical vector beams: from mathematical concepts to applications. *Adv. Opt. Photon.* **1**, 1-57 (2009).
- 29 Lai, G. & Yatagai, T. Generalized phase-shifting interferometry. *J. Opt. Soc. Am. A* **8**, 822-827 (1991).
- 30 Fienup, J. R. Phase retrieval algorithms: a comparison. *Appl. Opt.* **21**, 2758-2769 (1982).

End Notes:

Acknowledgements

This work was supported by KAIST, BK21+ program, Tomocube, and National Research Foundation of Korea (2015R1A3A2066550, 2014M3C1A3052567, 2014K1A3A1A09063027). I would like to thank Kitak Kim and Wonjune Choi for the fruitful discussions and comments.

Author Contributions

K.-R.L. developed the theory, performed the experiments, and analyzed the data. Y.P. conceived and supervised the project. K.-R.L., and Y.P. wrote the manuscript.

Competing financial interests

K.-R.L. and Y.P. are inventors on a patent describing a method for direct holography. (Republic of Korea patent application number 10-2016-0043274).